DOI: 10.1021/cg1005105

CRYSTAL GROWTH & DESIGN Article

2010, Vol. 10
3956–3963

Growth Modification of Seeded Calcite by Carboxylic Acid Oligomers and Polymers: Toward an Understanding of Complex Growth Mechanisms

Ulrich Aschauer,* Johannes Ebert, Anne Aimable, and Paul Bowen

Laboratoire de technologie des poudres (LTP), IMX/STI/EPFL, Station 12, 1015 Lausanne, Switzerland

Received April 16, 2010; Revised Manuscript Received July 8, 2010

ABSTRACT: Polycarboxylate molecules and oligomers have been investigated as growth modifiers during seeded calcite precipitation. To better understand possible molecular interactions and kinetic effects, additives with different structures and molecular weights have been investigated in this work. All additives show growth modifying effects, albeit less strongly for succinic acid and glutaric acid. This is attributed to a relatively weak interaction with the precipitated particles as well an additive size too small to influence the aggregation phase of the growth mechanism. Poly(acrylic acid) and poly(aspartic acid), on the other hand, led to strong growth modification, with the resulting particles being nanostructured, formed by an assembly of nanosized primary particles and consequently having a high specific surface area. Poly(aspartic acid) showed a stronger growth modifying effect than poly(acrylic acid) at a similar molecular weight and functional group concentration. This was not readily explainable without using molecular dynamics simulations (reported in a separate article), which suggests that the differences originate from the rigidity of the backbone and favorable electrostatic interactions between backbone nitrogen atoms and the surface in the case of poly(aspartic acid).

1. Introduction

Calcium carbonate is an important material for many industrial applications requiring specific phases, particle sizes, and morphologies. The occurrence of calcium carbonate in many living organisms has also led to much attention toward biomimetic synthesis of $CaCO_3$, trying to understand the growth mechanisms leading to the very particular morphologies observed in nature.[1,2] Besides reaction conditions such as pH and temperature, organic molecules or biopolymers, which are frequently present during the natural synthesis of calcite, are known to strongly modify crystal growth. The identification of systematic effects aimed toward understanding the underlying growth modifying mechanism induced by these natural or similar synthetic additives is therefore a field of great interest. This is reflected by the vast number of related publications during recent decades.

At high supersaturation, calcite is believed to grow by aggregation of smaller subunits, with the exact mechanism being dependent on the amount of additive present on the subunit surfaces.[3,4] The use of calcite seeds[5] effectively avoids the formation of precursor phases[6] such as vaterite,[3] giving directly calcite particles. At submonolayer additive concentrations, these small calcite particles undergo oriented self-assembly due to attractive interparticle forces.[4] These aggregates then ripen to seemingly single-crystals, imperfections in the self-assembly becoming pores, in which the additive is trapped.[7−9] Additive concentrations of more than a monolayer have a 2-fold effect. On one hand, oriented self-assembly is suppressed by steric repulsion forces, and on the other hand, growth sites are blocked by the additive. This leads to random aggregation of small additive coated particles, which undergo only limited ripening, resulting in particles with a high specific surface area.[4]

The molecular weight has been identified as one of the important factors for effective growth modification. Small polyanions have different degrees of influence depending on their structure.[10] Some, such as tartaric acid, have been claimed to influence only nucleation but not growth,[11] while larger macromolecules, such as double-hydrophilic block copolymers,[12−14] polyamino acids,[15−20] as well as polycarboxylic acids,[3,21−28] were seen to significantly influence the growth of calcium carbonate. The effect of the molecular weight can be 2-fold. On one hand, a smaller additive will have a higher diffusion coefficient and may therefore bind more rapidly to calcite particles. On the other hand, a short additive has a smaller number of functional groups, limiting the anchor-point density, the binding energy, and thus the residence time on the particle surface. This implies that while shorter additives are likely to bind to the surface faster, they may form a layer too thin to prevent particle agglomeration. Moreover, once bound, they are likely to move on the surface by desorption and readsorption, which reduces the effective blocking of growth sites.

In the context of the growth model outlined above, the following additive size dependent mechanism can be suggested. A short additive will cover the primary particles very rapidly; however, their steric effect is not sufficient to suppress oriented self-assembly, nor do they block growth sites long enough to suppress a certain degree of ripening. A small additive may therefore influence the growth morphology in slow crystallizing systems[10] but will be less effective than polymeric molecules with longer residence times. On the other hand, a large additive, oligomer or polymer, will take some time to bind to surfaces, thus allowing a number of particles to undergo oriented self-assembly. Subsequently, additive

*To whom correspondence should be addressed. Present address: Princeton University, Chemistry Department, Frick Laboratory, Room 213, Princeton, NJ 08544. Telephone: +1-609-258-0116. Fax: +1-609-258-6746. E-mail: aschauer@princeton.edu.

 Published on Web 07/22/2010

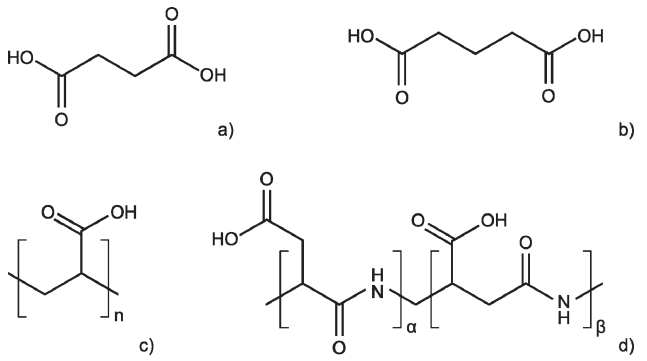

Figure 1. Molecular structure of the carboxylic acids used in the present study: (a) succinic acid; (b) glutaric acid; (c) poly(acrylic acid); and (d) poly(aspartic acid).

covered particles will attach to this self-assembled agglomerate in a random fashion, resulting in a particle with a dense core and a nanostructured shell of high specific surface area, as illustrated in a previous study using poly(acrylic acid).[4]

The goal of the present work is to study the effect of molecular weight in a systematic way in order to support the above hypothesis. Additives used in this work carry carboxylic acid functional groups, the degree of deprotonation and thus the activity of which is determined by the pH.[12,21] These additives are known to be very effective growth modifiers for many crystalline systems.[26,29−33] It was pointed out that while calcite growth is strongly affected, nucleation was not influenced by the presence of carboxylic acids, which was explained by a stronger affinity for the calcite crystals than for free calcium ions.[22] Surface complexation of the calcite phase by mono-, di-, and tricarboxylates has been investigated,[23] and it was found that carboxylic acids with one acid group did not bind to the surface, whereas two and three acid group oligomers did, which implies that simple electrostatic interaction is not the sole reason for binding. It was suggested that pairs of carboxylic acid groups complex surface calcium ions, thus making it possible to apply the results from complexation of calcium ions in solution[34−36] to surfaces.

The additives investigated in this study are poly(acrylic acid) (PAA; Figure 1c) as well as the monomers succinic acid (SA; Figure 1a) and glutaric acid (GA; Figure 1b). It was found that at sufficiently high concentrations PAA is able to completely inhibit precipitation, which was not achieved for shorter molecules.[27] The additive was shown to have different effects at different temperatures, resulting in rounded particles at room temperature whereas cubes were formed at 80 °C.[21] The same authors also showed that the effect of the additive is most beneficial at pH 10−11, with lower pH showing only little influence, most likely due to insufficient deprotonation, whereas a higher pH results in chaotic morphologies. A growth mechanism based on the aggregation of small primary particles has been suggested,[3,5] with the second reference showing incorporation of the polymer into the particle.

Other factors affecting the growth of calcite in the presence of additives were identified to be the hydrophilic/hydrophobic structure of the polymer and its general molecular structure.[12,14] Poly(aspartic acid) (p-ASP; Figure 1d) was therefore chosen as a fourth additive in the present work to investigate the effect of the backbone on growth modification of calcite. Moreover, p-ASP is a polyamino acid, which is present in many biomineralization processes, making it an interesting additive to investigate biomimetic growth modification. The additive was shown to influence the growth of calcite[17−20,37] as well as its dissolution;[15,16,38,39] however, the underlying mechanisms are not fully understood. It was suggested that p-ASP binds to step edges,[17,37] where it could very effectively suppress growth. Although this work was carried out at low supersaturations, the binding mechanism can be expected to be similar at higher supersaturations even if agglomeration kinetics may limit the effect at early stages of precipitation. The former reference[17] shows that low molecular weight p-ASP (up to two monomer units) binds to acute step edges whereas higher molecular weight additives preferentially bind to obtuse steps, the reason being that the energy required for the dehydration of an acute step is larger than the binding energy for longer molecules.

As can be seen from the existing literature cited above, carboxylate growth modifiers have been used extensively to influence calcite morphologies. However, often only a single molecule is used per study, making it difficult to conclude on systematic effects as a function of molecule type, chain length, additive concentration, degree of functional group dissociation, pH, and ionic composition of the medium. To overcome this shortcoming, the present work compares the influence of the monomers succinic acid (SA; Figure 1a) and glutaric acid (GA; Figure 1b) as well as the polymers poly(acrylic acid) (PAA; Figure 1c) and poly(aspartic acid) (p-ASP; Figure 1d) on the seeded precipitation of calcite. The selected additives allow on one hand the study of the effect of molecular weight (SA, GA, PAA) as well as the backbone (PAA, p-ASP) to try and elucidate possible systematic kinetic and binding strength effects discussed in the above growth models. The precipitates have been characterized by their particle sizes, morphologies, and specific surface areas. Synthesis of the pure calcite phase is ensured by the seeding technique previously described.[5] The seeding also limits the effects of such additives on the prenucleation clusters, where the different roles of complexation, cluster stabilization, and growth inhibition have recently been discussed.[40] We have reported in a separate article[41] theoretical investigations using molecular dynamics simulations, which have been carried out in parallel on these calcite/additive systems. This combined experimental and theoretical approach allows us to gain a better fundamental understanding of the adsorption behavior of organic additives on calcite and the resulting growth modifying effects.

2. Materials and Method

All precipitation experiments were carried out by mixing of aqueous solutions of calcium nitrate (Fluka, No. 21195) and potassium carbonate (Fluka, No. 60110) at 0.02 M prepared with ultrapure water (0.055 μS/cm with membrane filtration at 0.2 μm). The additives succinic acid (Acros, CAS 110-15-6), glutaric acid (Acros CAS 110-94-1), poly(acrylic acid) (MW 2000: Aldrich, CAS 9003-01-4, MW 5000: Acros, CAS 9003-01-4, MW 10000: commercial solution Dispex A40 from Ciba), and poly(aspartic acid) (MW 500 and MW 1000: synthesized at the Max-Planck-Institute for Colloids and Interfaces, Golm, Germany; MW 2100: Sigma, CAS 94525-01-6) were added to the potassium carbonate solution.

The ratio R between the concentration of deprotonated carboxylic acid groups and the concentration of calcium ions (0.01 M in the reaction mixture) has been used to normalize the results of the different additives, making them directly comparable. The concentration of deprotonated acid groups has been estimated from the mass fraction of polymer, the chain length, and the degree of deprotonation at the pH of the

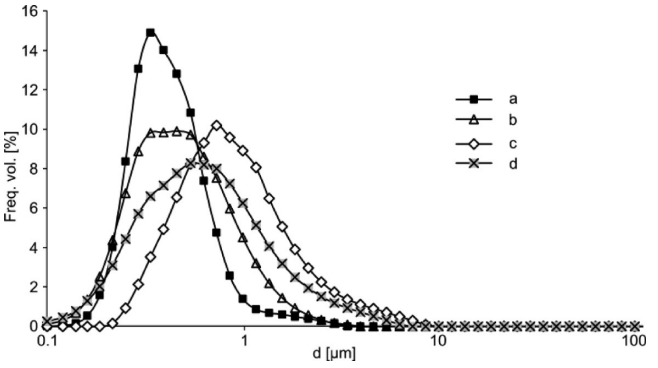

Figure 2. Particle size distributions obtained in the presence of (a) the Y mixer + 20 cm tube, (b) the Y mixer only, (c) a double jet with mixing below the suspension surface in the reactor, and (d) a double jet with mixing above the suspension surface in the reactor.

precipitation reaction (8−9) considered in the present work. The degrees of deprotonation considered were a full deprotonation for SA, GA, and p-ASP and a partial deprotonation of 0.815 for PAA.[42]

A small amount (0.5 g/L) of calcite seed source particles (pure calcite with a specific surface area of 35 m^2/g and $D_{v,90} < 1$ μm, as described elsewhere[5,43]) was suspended in the potassium carbonate solution. The suspension was treated in an ultrasonic bath for 5 min in order to detach seed particles from the surface and was then filtered through a 0.2 μm membrane (Nalgene, Cat. No. 190-2520), removing the parent (seed source) particles. The resulting suspension contained thus solely particles smaller than 200 nm, with the actual size of the detached pure calcite seed particles being estimated at 8 nm (number density: 2−16 seeds/μm^3). Up to now, the characterization of the seed size and number density can only be performed indirectly by calculations of seed-solubility and not directly by methods such as cryogenic-TEM or PCS, as discussed in detail in a previous study.[5] The calcium nitrate solution was filtered with the same type of membrane to remove impurities, which could otherwise serve as heterogeneous nucleation sites, promoting the formation of other phases.

Mixing was carried out in a 20 mL minibatch reactor with a computer controlled syringe injection system composed of two 10 mL syringes. The two flows were injected at ambient conditions into a Y mixer leading to a 20 cm tube for intense mixing before arriving in the reactor. This setup was found to give the smallest, narrowest, and most reproducible particle size distribution when compared to other geometries, such as direct injection into the reactor or using the Y mixer only (Figure 2).

After mixing, the suspension was allowed to age in the reactor for 15 min at ambient temperature (pH of the supernatant 8−9) before being either analyzed using laser diffraction (Malvern Mastersizer S) or filtered using a 0.2 μm membrane filter. Particles were then washed with 100 mL of ultrapure water, before being dried in a silica gel desiccator for about 10−24 h. Further analysis was made on the dry powder: powder X-ray diffraction (XRD, Siemens Kristalloflex 805), nitrogen adsorption leading to the specific surface area S_{BET} using the BET model (Micromiretics Gemini 2375), ζ potential (Brookhaven Zeta Pals), thermogravimetric analysis (TGA, Mettler Toledo TGA/SDTA 851e), and electron microscopy (SEM, Philips XLF 30; TEM, Philips CM 200). The span of the particle size distribution was calculated according

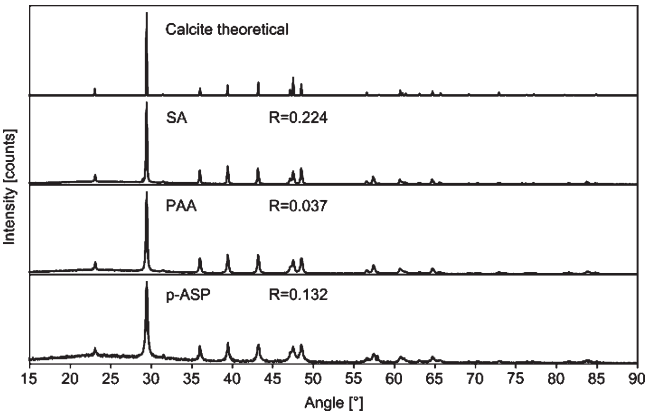

Figure 3. XRD spectra for calcite synthesized in the presence of succinic acid (SA), poly(acrylic acid) (PAA), and poly(aspartic acid) (p-ASP) compared to the theoretical spectrum of calcite as calculated from its crystal structure.

to eq 1, and the agglomeration factor was evaluated as given in eq 2.[44]

$$\text{span} = \frac{D_{v,90} - D_{v,10}}{D_{v,50}} \quad (1)$$

$$F_{ag} = \frac{D_{v,50}}{D_{BET}} = \frac{D_{v,50} S_{BET} \rho}{6} \quad (2)$$

$D_{v,10}$, $D_{v,50}$, and $D_{v,90}$ are the equivalent volume spherical diameters. The density of calcite is $\rho = 2.710$ g/cm^3, and S_{BET} is the specific surface area as determined after drying at 200 °C under flowing nitrogen.

The XRD peak broadening allows us to determine the size of the primary crystallite, d_{XRD}, using the Scherrer equation (eq 3)

$$d_{XRD} = \frac{K\lambda_X}{\beta_{Xp} \cos(\Theta)} \quad (3)$$

where K is equal to 0.9, λ_X is the X-ray wavelength, and β_{Xp} is the integral breadth of the material. For a limited series of samples, specific surface areas were measured after a thermal treatment at 350 °C in air for 2 h to remove any adsorbed additives (see the TGA results for the choice of temperature). The heat treatment was confirmed to affect neither the morphology (SEM) nor the crystallite size (XRD peak broadening).

In order to predict the steric barriers created by the different additives and estimate their effect on the aggregation phase of growth, interparticle interaction calculations were performed using the Hamaker 2.0 software, which was developed in-house and is publicly available.[45] This software evaluates the total interparticle interaction within the DLVO theory[46,47] as a combination of dispersion, electrostatic, and steric interaction models published in the literature. The models used in the present case were the Vincent[48] approach for dispersion interactions, the Hogg−Healy−Fürstenau[49] approach for electrostatic interactions as well as Bergstrom's[50] approach for the steric interactions. Common parameters used are a ζ potential of 7 mV and an aqueous solution containing ions of valence 1 at a concentration of 0.001 M as dispersion medium. The Hamaker constant[51] used is 1.44×10^{-20} J, and all calculations were done for room temperature. The electrostatic origin was fixed at the outside of the adsorbed layer, which was 0.1 nm for water and the adsorbed layer thickness in the presence of a polymer. The variable parameters used in

Table 1. Particle Size ($D_{v,50}$ and Span), ζ Potential and Specific Surface Area (SSA) and the Resulting Equivalent Diameter (D_{BET}), Agglomeration Factor (F_{ag}), Yield, and Supersaturation (S) at the Beginning of the Reaction ($t = 0$) of Powders Obtained in the Presence of Succinic Acid and Glutaric Acid at Different Concentration Ratios R

	R	$D_{v,50}$ (μm)	span	ζ (mV)	SSA (m^2/g)	D_{BET} (μm)	F_{ag}	yield (%)	S ($t = 0$)
succinic acid (SA)	0.084	0.94	3.10	−24	5.7	0.39	2.41	83.5	29
	0.224	1.13	1.07	−29	5.1	0.43	2.60	61.9	23
	0.440	2.01	1.79	−31	4.2	0.53	3.81	46.3	21
glutaric acid (GA)	0.224	1.20	1.43	−26	4.3	0.51	2.33		23
	0.440	2.10	2.20	−29	4.7	0.47	4.46		21

the different calculations are given with the results in the next section.

3. Results and Discussion

X-ray diffraction (XRD) analysis (Figure 3) confirmed calcite was the only precipitated phase for all types of additives, showing the effectiveness of the seeding approach to avoid the formation of vaterite, often observed under similar reaction conditions without seeds.[5] We note that the broad hump at low angles, especially for p-ASP, is due to the glass sample holder appearing, due to the relatively small sample size and not due to an amorphous phase.

3.1. Succinic Acid (SA) and Glutaric acid (GA). Table 1 gives the particle size, ζ potential, and specific surface area of the powders obtained in the presence of SA and GA. The magnitude of the ζ potential slightly increases with increasing concentration ratio R, which can be explained by an increased concentration of charged additive at the surface, as seen for other carboxylates on calcite.[52]

It can be seen that an increased additive concentration is accompanied by an increase in particle size. This could be due to a modification of the aggregation versus growth mechanisms, as these molecules are known to affect single crystal growth[10] but are expected to only have a small influence on aggregation, as shown below. The chemical composition of the solution at the initial stage of the reaction was determined using solubility calculations,[23,42,53] and the supersaturation ratio S at $t = 0$ is reported in Table 1. There is a small decrease of the supersaturation at $t = 0$ with increasing R, due to an increasing complexation of calcium ions with these small carboxylic acids. This effect is more important with SA, whereas it is only minor with GA. The huge decrease in yield observed with increasing R could not be explained thermodynamically, as the amount of calcium ions available for the precipitation reaction remains in the same range. Kinetic effects via an interaction with prenucleation clusters, as observed for citric acid,[40] could be at the origin of the decrease in yield, as all precipitates were allowed to age for only 15 min. This could also explain the apparent low influence of tartaric acid on the growth of calcite[11] despite its relatively strong adsorption onto calcite powders.[52]

For SA, one observes a small decreasing trend of the specific surface area with increasing R, while for GA only little influence with variations within the experimental error (±0.4 m^2/g) is seen. It was observed that aging of the suspension containing the seeds prior to precipitation yielded a broader distribution with a similar $D_{v,50}$, suggesting agglomeration of the seeds. This implies that the additives do not form a sufficient steric barrier between seed particles, which could be due to the additives insufficient size or low adsorbed amount,[4] as shown in the thermogravimetric (TGA) results presented below. To verify this hypothesis, interparticle interaction calculations were performed for both additives at particle sizes of 40 and 90 nm (primary particle sizes observed in previous work with PAA[5]). The only variable was the thickness of the adsorbed layer, for which the extreme values of the molecule either flat (SA = 0.38 nm, GA = 0.41 nm) on the surface or fully upright (SA = 0.41 nm, GA = 0.62 nm) were considered. The resulting curves are shown in Figure 4. It can be seen that for all cases these small additives cannot reduce the depth of the primary minimum to less than $2kT$ (GA) or $4kT$ (SA) even in the maximum layer case and can thus not prevent agglomeration. Similar calculations for PAA[4] showed the minimum to disappear, thus stabilizing the particles, which is also expected to be the case for p-ASP.

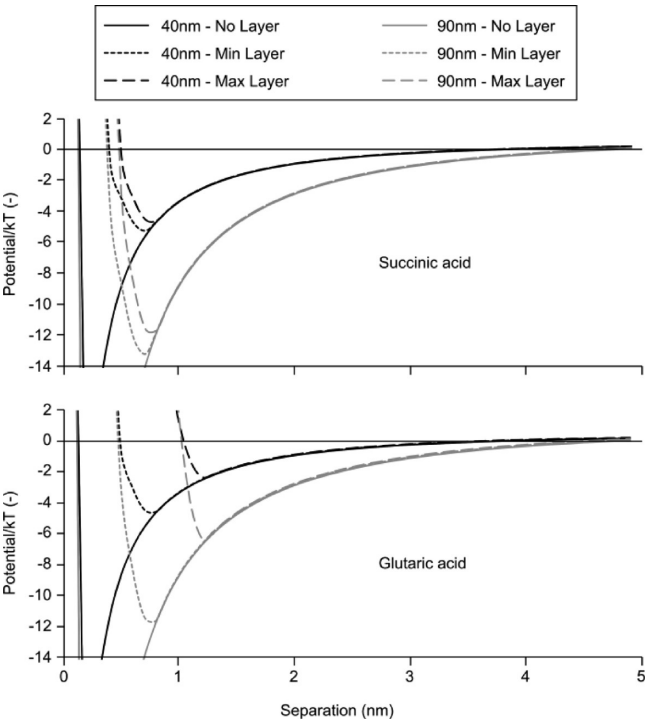

Figure 4. Calculated interaction potentials for glutaric acid (top) and succinic acid (bottom). For each additive, the potentials were calculated for 40 nm (black) and 90 nm (gray) particles, while considering the particle either without additive (solid) or with a flat adsorbed additive = min layer (short dash) and an upright adsorbed molecule = max. layer (long dash).

Scanning electron microscopy (SEM) analysis (Figure 5) revealed the particles to be made up of prismatic subunits, presumably of the stable $(10\bar{1}4)$ face of calcite. This morphology and the surface areas are similar to those found with low concentrations (submomonlayer) of polymers[4] and oligomers, and particles appear as single crystals in electron diffraction.[4] The morphology is different to that observed for slow crystal growth at low supersaturations in the presence of SA,[10] which is linked with the much quicker growth kinetics in our study and will be discussed in more detail below.

TGA analysis for calcite precipitated in the presence of succinic acid (Figure 6) showed no detectable residual additive at the surface of the filtered particles. This fact implies that these short additive molecules do not bind strongly enough to the surface to remain there long enough to have a large effect on the growth at the high supersaturations used in this study. This is strongly supported by our molecular dynamics calculations performed with these two additives.[41] We found that these small molecules rapidly explore a manifold of configurations around the investigated acute growth step. This is true even in the time window of our molecular dynamics calculations of a few nanoseconds. Therefore, at the considered supersaturations, these small molecules have a weak effect on growth morphology due to the aforementioned kinetic considerations. For the p-ASP samples, a 5% weight loss is seen around 300 °C, indicating adsorbed polymer on the particle after washing and drying.

3.2. Poly(acrylic Acid) (PAA): Effect of the Concentration Ratio *R* and Molecular Weight MW. For PAA, four different concentration ratios *R* and three different molecular weights (MWs) were investigated: the characteristics of the obtained particles are given in Table 2.

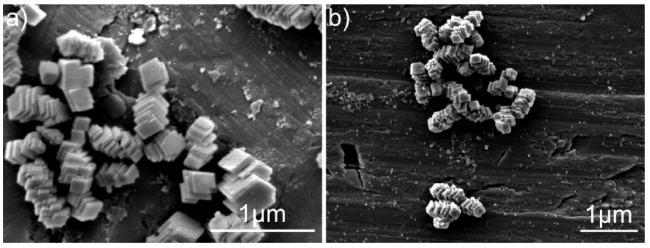

Figure 5. Scanning electron micrographs showing the morphologies obtained (a) in the presence of succinic acid, $R = 0.224$, and (b) in the presence of glutaric acid, $R = 0.224$.

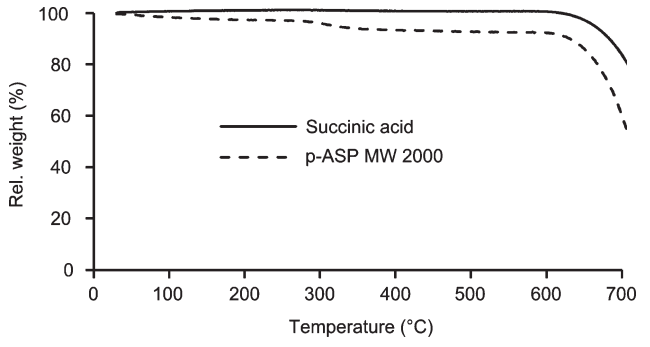

Figure 6. TGA profile of SA and MW 2000 p-ASP modified calcite. The weight loss above 630 °C is attributed to calcite decomposition.

Aging the seed and PAA 2000 containing suspension did not show any influence on the particle size distribution, indicating that the PAA 2000 adsorbs onto the seeds, forming a sufficiently high steric barrier to prevent their agglomeration.[4] As with the simple acids, a higher *R* results in a lower yield, indicating that PAA forms stable complexes with the calcium ions in solution, as previously reported.[34−36] This was also observed in our molecular dynamics simulations,[41] where the complexation modified the adsorbed conformation and reduced the effectiveness of PAA as a growth modifier. This "trapping" of calcium ions ultimately prevents them from taking part in the reaction, thus decreasing the yield. Experimentally, the precipitation carried out at a high concentration ratio $R = 0.22$ with PAA 2000 was greatly slowed down, and almost no precipitate was obtained after the regular aging time of 15 min (results presented here are those of the powder obtained after 2 h). With the same ratio, $R = 0.22$, and PAA 5000, no powder could be obtained, even after several hours of aging, indicating a strong inhibition of precipitation.[27] However, no effect on the precipitation kinetics was observed when using PAA with a higher molecular weight of 10000.

As can be seen from the data in Table 2, the particle size of powders precipitated with PAA 2000 does not vary much for different $R < 0.11$; however, the specific surface area and thus the agglomeration factor increase notably with increasing *R*. PAA 2000 thus seems to attach strongly enough to hinder growth but not stop agglomeration, leading to agglomerated particles made up from smaller primary particles, as indicated by the XRD crystallite size d_{XRD} (Table 2). A higher additive concentration ($R = 0.22$) leads to a lower specific surface area, indicative of a reduced inhibition of crystal growth. This can be related to modified precipitation kinetics due to a decrease of the effective supersaturation by complex formation of calcium ions with the additive.[5] Also, our molecular dynamics simulations[41] showed that there was a significant entropic contribution to the adsorption energy for PAA. Complexation will also reduce the electrostatic contribution, decreasing the effective binding strength and residence time of PAA at the calcite surface.

Powders precipitated in the presence of higher molecular weight PAA, especially MW = 10000, present lower specific surface areas (SSAs) and larger crystallite sizes (d_{XRD}). This is true both before and after the thermal treatment to remove the polymer, which does have a significant effect on the SSA but does not influence the d_{XRD}. This result would suggest that PAA of higher molecular weight did not bind as strongly or in the same fashion during the final stage of calcite precipitation,[4] leading to a possible ripening. The primary particle size calculated by d_{XRD} decreases with increasing *R* for PAA of different molecular weights. This is coherent with

Table 2. Particle Size Distribution ($D_{v,50}$ and Span), ζ Potential, Specific Surface Area (SSA), and the Resulting Equivalent Diameter (D_{BET}), Agglomeration Factor (F_{ag}), Crystallite Size (d_{XRD}), and Yield at Different Concentration Ratios *R* for Different Molecular Weights (MWs) of Poly(acrylic Acid) (PAA)[a]

MW	*R*	$D_{v,50}$ (µm)	span	ζ (mV)	SSA (m^2/g)	D_{BET} (µm)	F_{ag}	d_{XRD} (µm)	yield (%)
2000	0.027	0.43	1.5	−33	30.3	0.07	5.3	0.034	85.9
2000	0.037	0.52	1.4	−36	36.2	0.06	6.5	0.036	79.3
2000	0.110	0.41	1.3	−40	45.3 (9.1)	0.05	7.7	0.039	63.1
2000	0.220[b]	2.42	10.51		32.8	0.07	34.6	0.026	
5000	0.110	0.53	15.80		27.5 (3.6)	0.08	6.6	0.030	
10000	0.110	0.36	1.55		19.1 (4.4)	0.11	3.3	0.069	
10000	0.220	0.34	0.76		16.5	0.13	2.6	0.049	

[a] SSA values in parentheses were measured after a thermal treatment at 350 °C for 2 h in air. The large spans observed for the MW 2000 and 5000 samples are due to residual agglomerates. [b] Obtained after 2 h of aging.

the model developed in ref 4, which proposes a calcite growth only on seeds, the number of which is determined by the PAA concentration linked to the colloidal stability of the seeds, as explained in detail in a previous study.[5] The d_{XRD} is higher, with MW = 10000 confirming its lower ripening inhibition properties.

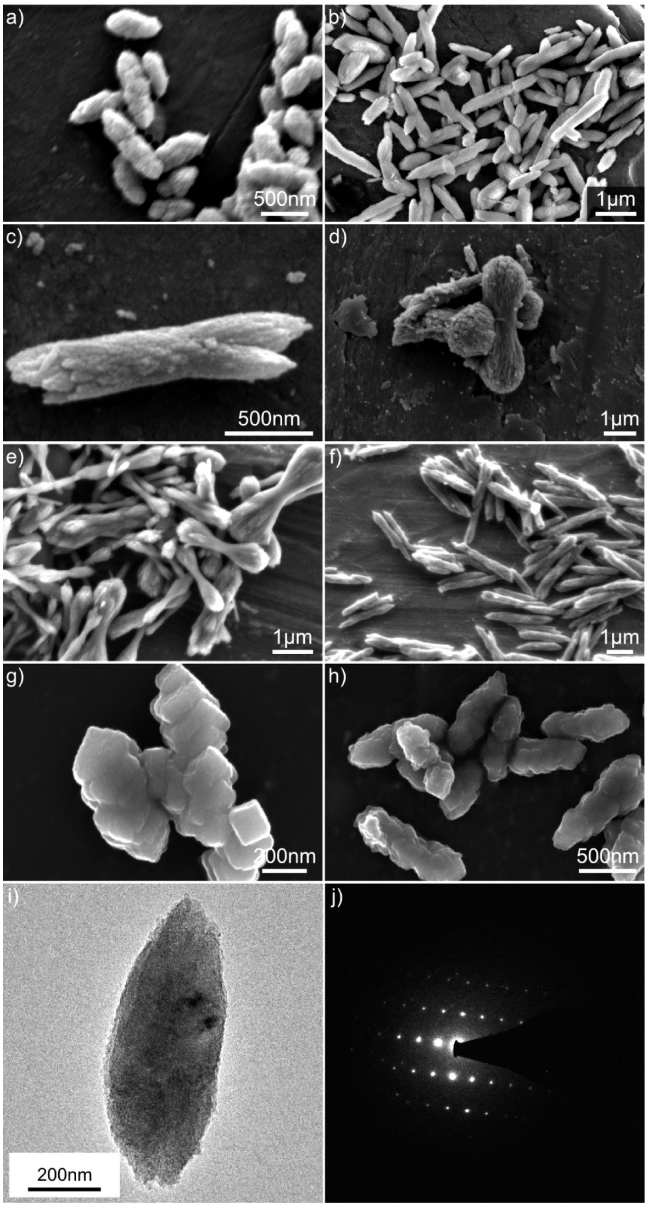

Figure 7. Calcite particles grown at different concentration ratios of PAA 2000: (a) $R = 0.027$; (b) $R = 0.037$; (c) $R = 0.11$; (d) $R = 0.11$; (e) $R = 0.22$. From pictures c−e the growth mechanism of the "dog-bone" morphology can be observed. PAA 5000: (f) $R = 0.11$. PAA 10000: (g) $R = 0.11$, (h) $R = 0.22$. (i) TEM bright-field image of PAA (MW = 2000, $R = 0.11$) and (j) electron diffraction pattern in the center of the particle.

SEM images of the powders are shown in Figure 7. It can be seen that the morphology is clearly no longer rhombic with increasing R but composed of agglomerated subunits resulting in a rough surface appearance. As R increases, the particles tend to show a "dog-bone" morphology. The morphology of the particles obtained with PAA 5000 is similar, resulting in elongated particles made of agglomerated subunits. On the contrary, the particles obtained with PAA 10000 are more platelets, with a lower aspect ratio, again confirming its lower ripening or growth inhibition capacity. From the electron diffraction pattern shown in Figure 7j it can be seen that the center of the particles does not consist of randomly agglomerated primary particles but rather a seemingly single crystal, strongly supporting the growth mechanism outlined in the introduction.

To compare the amount of PAA that can be adsorbed at monolayer coverage with the experimentally adsorbed amount from the TGA data, PAA was assumed to adsorb in a flat conformation with an occupied surface area of 0.7×6 nm^2 per 28 monomer additives. It was found that the ratio of experimental to theoretical adsorbed PAA MW 2000 was 0.64 and 0.78 for $R = 0.027$ and $R = 0.11$, respectively. These results show that the polymer does not completely cover the particles, however, with an increasing coverage with increasing R. With $R = 0.22$ the amount of adsorbed PAA is higher than the maximum theoretical amount needed to form a monolayer (0.75 mg of PAA per square meter[4]). This could indicate either that some PAA is "trapped" during crystal growth or that a mixed conformation is adopted by the PAA, e.g. "brush" rather than "pancake".[41]

The length of a polymer can have two effects. On one hand, the diffusion coefficient is likely to be higher for a shorter polymer, leading to more rapid adsorption kinetics. However, the number of functional groups attaching to the surface will determine the strength of the adsorption. As a longer molecule has a higher number of these anchor points, the binding will be stronger and desorption kinetics will be slower. From the above experimental data, it seems that the adsorption kinetics is the determining factor for growth inhibition, as PAA 2000 and 5000 have a more marked effect on the final crystal size, d_{XRD}, and morphology than PAA 10000.

3.3. Poly(aspartic Acid) (p-ASP) and Effect of Molecular Weight. For poly(aspartic acid), 3 different molecular weights of 5 monomers (MW ≈ 500), 10 monomers (MW ≈ 1000), and 20 monomers (MW ≈ 2000) were investigated at the same ratio R of 0.075 (Table 3). One experiment with the 20-monomer additive at $R = 0.15$ was carried out; however, the precipitation reaction was completely inhibited. The 20-monomer molecule has the same number of carboxylic acid groups as the PAA 2000 used previously.

Comparing this 20 monomer data to PAA 2000, we see that p-ASP is more effective at inhibiting growth of calcite, resulting in higher SSAs both before and after the polymer removal (70 cf. 40 m^2/g and 12.2 cf 9.1 m^2/g). It is known[17,37] that p-ASP can bind selectively to step edges, which are

Table 3. Powder Characteristics Obtained with Different Molecular Weights of p-ASP at $R = 0.075$[a]

monomers	R	$D_{v,50}$ (μm)	span	SSA (m^2/g)	D_{BET} (μm)	F_{ag}	d_{XRD} (μm)
5	0.075	0.55	4.41	6.70	0.33	1.66	0.129
10	0.075	0.89	5.98	38.15	0.06	15.40	0.060
20	0.075	0.59	20.00[b]	70.33 (12.2)	0.03	18.72	0.032

[a] The SSA value in parentheses was measured after a thermal treatment at 350 °C for 2 h in air. [b] Span is overestimated due to residual agglomerates of about 15 μm.

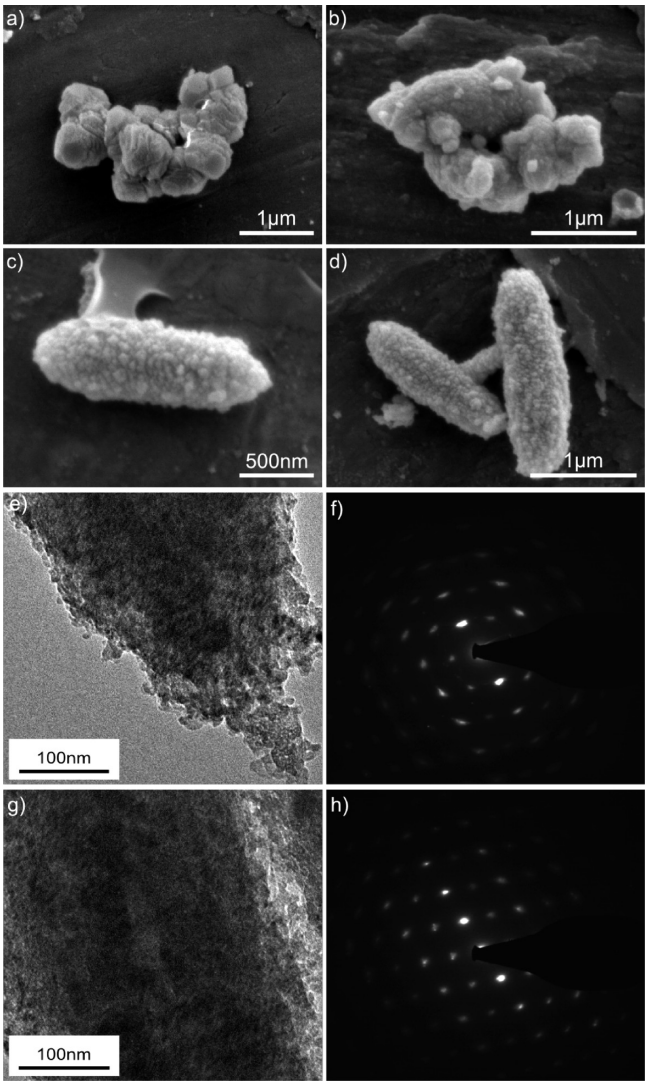

Figure 8. SEM micrographs of powders obtained at different molecular weights of poly(aspartic acid): (a) MW = 500, (b) MW = 1000, (c and d) MW = 2000, (e) TEM image at the border of the particle (MW = 2000), (f) electron diffraction pattern at the same location, (g) TEM image in the center of the particle (MW = 2000), and (h) electron diffraction pattern at the same location.

growth sites, thus blocking the growth and explaining to some degree the smaller primary particle size d_{XRD} (Table 3). The results suggest that PAA binds either less selectively or not as strongly, which would result in larger primary particles. Our theoretical molecular dynamics simulations[41] support the latter, as favorable electrostatic interactions existed only for the p-ASP backbone containing nitrogen atoms, leading to a higher adsorption energy.

SEM pictures (Figure 8) show a clear transition from the blocky structure close to the one obtained with the succinic and glutaric acids for only 5 monomers toward a highly nanostructured particle in the presence of longer molecules. The crystallite size d_{XRD} measured by XRD line broadening also shows a similar trend, with the crystallite size decreasing from around 130 nm to 60 and 30 nm as the molecular weight increases. The rather well-defined electron diffraction patterns (Figure 8f and g) show that oriented self-assembly also occurs in the case of p-ASP. Interestingly, at the particle surface (Figure 8f), the diffraction pattern tends toward the ring structure typical of an amorphous phase, indicating less orientation. This supports the meso-crystals[54] growth mechanism, outlined in the Introduction, by which, during the final stages of precipitation, additive coated particles attach in a random fashion to particle cores previously formed by oriented self-assembly.

As with poly(acrylic acid) , there seems to be a competition between the adsorption kinetics and the strength of adsorption, related to the number of functional groups which can create anchor points. From the above experimental data it seems that the number of anchor points is the determinant factor for growth inhibition, as growth modification by poly(aspartic acid) with 5 monomers is less marked than that for the 10 and 20 monomer cases. The fact that a large amount of additive adsorbs to the surface is also supported by the TGA data in Figure 6, where a weight loss of approximately 5% can be attributed to the additive.

Calcite with the highest specific surface area, indicating the most effective growth modification, is thus observed for carboxylic acid polymers of molecular weight between 2000 and 5000 g/mol, and at a concentration ratio of 0.11. A more in depth analysis of the marked differences between PAA and p-ASP based on theoretical molecular dynamics simulations is presented in a separate article.[41] The main difference was in the favorable electrostatic interaction with the nitrogen containing backbone of the p-ASP and the different complexation behavior of the two molecules. These simulation results indicate that there was a more rapid adsorption and longer residence times for the p-ASP at calcite surfaces, which can explain the higher specific surface areas of calcite grown in the presence of p-ASP compared to PAA.

4. Conclusions

Seeded precipitation of calcite was carried out in the presence of the two simple carboxylic acids, succinic acid (SA) and glutaric acid (GA), as well as the polymers poly(acrylic acid) (PAA) and poly(aspartic acid) (p-ASP) of different molecular weights. The resulting particles were characterized by looking at particle size, specific surface, X-ray diffraction, and ζ potential. All the additives had an effect on the particle morphology.

SA and GA had weaker effects on the particle size, specific surface area, ζ potential, and morphology when compared to the polymers and oligomers. This indicates that the binding between the particle and the molecule was not strong enough to result in long enough residence times to more strongly modify growth, which is in agreement with molecular dynamic simulations. Moreover, aging of the seed/additive containing suspension prior to precipitation gave broader particle size distributions, which can be explained by seed agglomeration due to the insufficient steric barrier formed by these rather small molecules. However, the precipitation yield decreased with increasing additive concentration, which thermodynamic calculations demonstrated was not due to calcium complexation. A possible reason may be due to a kinetic effect for these simple acids via an interaction with prenucleation calcite clusters.

PAA has a strong effect on the specific surface area and particle substructure, as previously reported. The growth modifying effect decreased as the molecular weight increased from 2000 to 10000. The growth or ripening inhibition by p-ASP was more pronounced than that for PAA, resulting in an even higher specific surface area. However, shorter molecules of p-ASP did not show such a strong growth modifying

effect, suggesting an optimum molecular weight between 2000 and 5000 for these types of polycarboxylates, where the adsorption strength and conformation influence the residence time of the molecules at the growing crystal surface. Our theoretical molecular dynamics simulations reported separately[41] support this hypothesis. They show that the differences between PAA and p-ASP originate from the rigidity and the chemistry (presence of nitrogen) of the backbone, which results in a more stable complex formation of PAA, rendering it less active, and a stronger binding of p-ASP, leading to a different adsorption conformation and more marked growth modification.

Acknowledgment. The authors are very grateful to Helmut Cölfen and Hans G. Börner at the Max-Planck-Institute for Colloids and Interfaces, Golm, Germany, for providing poly(aspartic acids) MW ~500 and ~1000 used in this study. Also Carlos Morais, Simone Pedrazzini, and Nicholas Ruffray are acknowledged for experimental help.

References

(1) Mann, S. *Nature* **1993**, *365*, 499.
(2) Mann, S.; Ozin, G. A. *Nature* **1996**, *382*, 313.
(3) Rieger, J.; Frechen, T.; Cox, G.; Heckmann, W.; Schmidt, C.; Thieme, J. *Faraday Discuss.* **2007**, *136*, 265.
(4) Donnet, M.; Aimable, A.; Lemaitre, J.; Bowen, P. *J. Phys. Chem. B*, in press.
(5) Donnet, M.; Bowen, P.; Jongen, N.; Lemaitre, J.; Hofmann, H. *Langmuir* **2005**, *21*, 100.
(6) Gower, L. B. *Chem. Rev.* **2008**, *108*, 4551.
(7) Wang, T. X.; Cölfen, H.; Antonietti, M. *J. Am. Chem. Soc.* **2005**, *127*, 3246.
(8) Judat, B.; Kind, M. *J. Colloid Interface Sci.* **2004**, *269*, 341.
(9) Schwahn, D.; Ma, Y. R.; Cölfen, H. *J. Phys. Chem. C* **2007**, *111*, 3224.
(10) Mann, S.; Didymus, J. M.; Sanderson, N. P.; Heywood, B. R.; Samper, E. J. A. *J. Chem. Soc., Faraday Trans.* **1990**, *86*, 1873.
(11) Prevost, A.; Butler, M. F.; Heppenstall-Butler, M. In *16th International Symposium on Industrial Crystallization*; VDI: Dresden, 2005; Vol. 1901, p 739.
(12) Cölfen, H.; Qi, L. M. *Chem. Eur. J.* **2001**, *7*, 106.
(13) Kaluzynski, K.; Pretula, J.; Penczek, S. *J. Polym. Sci., Part A: Polym. Chem.* **2007**, *45*, 90.
(14) Rudloff, J.; Antonietti, M.; Cölfen, H.; Pretula, J.; Kaluzynski, K.; Penczek, S. *Macromol. Chem. Phys.* **2002**, *203*, 627.
(15) Burns, K.; Wu, Y. T.; Grant, C. S. *Langmuir* **2003**, *19*, 5669.
(16) Wu, Y. T.; Grant, C. *Langmuir* **2002**, *18*, 6813.
(17) Elhadj, S.; Salter, E. A.; Wierzbicki, A.; De Yoreo, J. J.; Han, N.; Dove, P. M. *Cryst. Growth Des.* **2006**, *6*, 197.
(18) Volkmer, D.; Fricke, M.; Huber, T.; Sewald, N. *Chem. Commun.* **2004**, 1872.
(19) Teng, H. H.; Dove, P. M.; Orme, C. A.; De Yoreo, J. J. *Science* **1998**, *282*, 724.
(20) Didymus, J. M.; Mann, S.; Benton, W. J.; Collins, I. R. *Langmuir* **1995**, *11*, 3130.
(21) Yu, J. G.; Lei, M.; Cheng, B.; Zhao, X. J. *J. Solid State Chem.* **2004**, *177*, 681.
(22) Wada, N.; Kanamura, K.; Umegaki, T. *J. Colloid Interface Sci.* **2001**, *233*, 65.
(23) Geffroy, C.; Foissy, A.; Persello, J.; Cabane, B. *J. Colloid Interface Sci.* **1999**, *211*, 45.
(24) Westin, K.; Rasmuson, A. C. *J. Colloid Interface Sci.* **2005**, *282*, 359.
(25) Westin, K. J.; Rasmuson, A. C. *J. Colloid Interface Sci.* **2005**, *282*, 370.
(26) Reddy, M. M.; Hoch, A. R. *J. Colloid Interface Sci.* **2001**, *235*, 365.
(27) Kato, T.; Suzuki, T.; Amamiya, T.; Irie, T.; Komiyama, N. *Supramol. Sci.* **1998**, *5*, 411.
(28) Mann, S.; Heywood, B. R.; Rajam, S.; Birchall, J. D. *Nature* **1988**, *334*, 692.
(29) Amjad, Z. *Langmuir* **1987**, *3*, 1063.
(30) Grases, F.; Garciaraso, A.; Palou, J.; Costabauza, A.; March, J. G. *Colloids Surf.* **1991**, *54*, 313.
(31) Ouyang, J. M.; Duan, L.; Tieke, B. *Langmuir* **2003**, *19*, 8980.
(32) Ouyang, J. M.; Zhou, N.; Duan, L.; Tieke, B. *Colloids Surf., A: Physicochem. Eng. Aspects* **2004**, *245*, 153.
(33) Borah, B. M.; Bhuyan, B. J.; Das, G. *J. Chem. Sci.* **2006**, *118*, 519.
(34) Axelos, M. A. V.; Mestdagh, M. M.; Francois, J. *Macromolecules* **1994**, *27*, 6594.
(35) Sinn, C. G.; Dimova, R.; Antonietti, M. *Macromolecules* **2004**, *37*, 3444.
(36) Molnar, F.; Rieger, J. *Langmuir* **2005**, *21*, 786.
(37) Orme, C. A.; Noy, A.; Wierzbicki, A.; McBride, M. T.; Grantham, M.; Teng, H. H.; Dove, P. M.; DeYoreo, J. J. *Nature* **2001**, *411*, 775.
(38) Teng, H. H. *Geochim. Cosmochim. Acta* **2004**, *68*, 253.
(39) Teng, H. H.; Dove, P. M. *Am. Mineral.* **1997**, *82*, 878.
(40) Gebauer, D.; Cölfen, H.; Verch, A.; Antonietti, M. *Adv. Mater.* **2009**, *21*, 435.
(41) Aschauer, U.; Spagnoli, D.; Bowen, P.; Parker, S. C. *J. Colloid Interface Sci.* **2010**, *346*, 226.
(42) Donnet, M. Ph.D. Thesis, EPFL, 2002.
(43) Jongen, N.; Donnet, M.; Bowen, P.; Lemaitre, J.; Hofmann, H.; Schenk, R.; Hofmann, C.; Aoun-Habbache, M.; Guillemet-Fritsch, S.; Sarrias, J.; Rousset, A.; Viviani, M.; Buscaglia, M. T.; Buscaglia, V.; Nanni, P.; Testino, A.; Herguijuela, J. R. *Chem. Eng. Technol.* **2003**, *26*, 303.
(44) Bowen, P. *J. Dispersion Sci. Technol.* **2002**, *23*, 631.
(45) Aschauer, U.; Burgos-Montes, O.; Moreno, R.; Bowen, P. *J. Dispersion Sci. Technol.*, in press, http://ltp2.epfl.ch/hamaker2.
(46) Derjaguin, B.; Landau, L. *Acta Phys. Chem. URSS* **1941**, *14*, 633.
(47) Verwey, E. J. W.; Overbeek, J. T. G. *Theory of the Stability of Lyophobic Colloids*; Elsevier: Amsterdam, 1948.
(48) Vincent, B. *J. Colloid Interface Sci.* **1973**, *42*, 270.
(49) Hogg, R.; Healy, T. W.; Fuerstenau, D. W. *Trans. Faraday Soc.* **1966**, *62*, 1638.
(50) Bergstrom, L.; Schilling, C. H.; Aksay, I. A. *J. Am. Ceram. Soc.* **1992**, *75*, 3305.
(51) Bergstrom, L. *Adv. Colloid Interface Sci.* **1997**, *70*, 125.
(52) Plank, J.; Bassioni, G. *Z. Naturforsch., Sect. B: Chem. Sci.* **2007**, *62*, 1277.
(53) Donnet, M.; Bowen, P.; Lemaitre, J. *J. Colloid Interface Sci.* **2009**, *340*.
(54) Cölfen, H.; Antonietti, M. *Mesocrystals and Nonclassical Crystallization*; John Wiley & Sons Ltd: Chichester, West Sussex, England, 2008.